TiO_2-Loaded WO_3 Composite Films for Enhancement of Photocurrent Density *

Wen-Gui Wang(王文桂), Li Zhu(朱丽), Yu-Yan Weng(翁雨燕)**, Wen Dong(董雯)**

College of Physics, Optoelectronics and Energy, Collaborative Innovation Center of Suzhou Nano Science and Jiangsu Key Laboratory of Thin Films, Soochow University, Suzhou 215006

(Received 5 October 2016)

Titanium dioxide (TiO_2) loaded tungsten trioxide (WO_3) composite films are prepared by an E-beam vapor system. Associated with the existence of a heterojunction at the interface of TiO_2 and WO_3, the prepared TiO_2-WO_3 composite film shows enhanced photocurrent density, four times than the pure WO_3 film illuminated under xenon lamp, and higher incident-photon-to-current conversion efficiency. By varying the initial TiO_2 film thickness, such composite structures could be optimized to obtain the highest photocurrent density. We believe that thin TiO_2 films improve the light response and increase the surface roughness of WO_3 films. Furthermore, the existence of the heterojunction results in the efficient charge carriers' separation, transfer process, and a lower recombination of electron-hole pairs, which is beneficial for the enhancement of photocurrent density.

PACS: 82.45.Mp, 81.05.Cy, 84.60.Jt DOI: 10.1088/0256-307X/34/2/028201

Semiconductor photocatalysis has been widely studied in the last few decades as one of the most effective techniques for a means to harvest and covert solar light to chemical energy.[1–6] Among these semiconductors, tungsten trioxide (WO_3) has been widely considered to be a photocatalytic material because of a proper band gap for visible light absorption ($E_g \approx 2.8$ eV) and high stability in aqueous solution under acidic conditions, no-photocorrosion.[7] However, for single semiconductor materials, there are still some drawbacks in the field of photocatalysis such as short photogenerated electron-hole pair lifetimes and the limited visible-light absorption.

Compared with these single semiconductor photocatalysts, a heterojunction photocatalyst, which contains two or more dissimilar semiconductors, generally offers more advantages in improving the photocatalytic activity.[8–12] The formation of a heterojunction between different semiconductors can drive the separation and transportation of the electron-hole pairs effectively. In addition, the coupling of semiconductors can also satisfy the higher absorption of solar energy. Among a wide variety of heterojunction systems, tungsten trioxide-titanium dioxide (WO_3-TiO_2) is one of the most studied systems.[13–17] As is known, titanium dioxide (TiO_2) has also been used as a most popular photocatalyst since Fujishima *et al.* first demonstrated that it is possible to produce hydrogen from water under UV irradiation.[18]

Many important findings have been reported on the WO_3-TiO_2 heterojunction photocatalysts during the past few years. For example, a higher photoresponse was observed for bilayered WO_3-TiO_2 composite films relative to single component films. Electron injection into the bulk WO_3 layer was invoked as a mechanism for reduced surface carrier recombination in the TiO_2 component in these composites.[19] In addition, the photocatalytic activity of WO_3-TiO_2 composite films was found to be three times higher than that of pure TiO_2 films for the gas-phase oxidation of 2-propanol.[20] A TiO_2 coating coupled with a WO_3 can be as an 'electron pool' in the design of a photoelectron-chemical anticorrosion system with built-in energy storage capability.[21]

As can be seen, the WO_3-TiO_2 heterojunction system is the subject of great interest for its excellent properties in photocatalysis and high stability. Many previous researches always focused on the TiO_2 film modification with WO_3. Thus inspired by these researches, we deposited a thin TiO_2 film onto a WO_3 layer followed by a thermal annealing to form composite TiO_2-WO_3 electrodes in this study. It is noted that a significant enhancement of the photocurrent density is readily obtained under white light, visible light and UV light illumination for the TiO_2-thin film loaded WO_3 composite system. Meanwhile, such heterojunction structures could be optimized by varying the initial TiO_2 film thickness to obtain the highest photocurrent density and generation efficiency.

The WO_3 film on the fluorine doped tin oxide (FTO) grass substrate was prepared by the E-beam vapor deposition method from WO_3 pieces (purity 99.99%, Kurt J. Lesker Company). Before deposition, the FTO grass (1 cm × 1.5 cm) was cleaned ultrasonically in the acetone, ethanol, and deionized water successively and then dried by a stream of N_2. Then, the samples were positioned on a disc at a distance of 200 mm from the vapor resource. Additionally, the chamber pressure was pumped down to 1×10^{-4} Pa, and then applied 5 kV high voltage to pre-melt the WO_3 target and TiO2 target. When these targets were bombarded by electrons and melted completely,

*Supported by the National Natural Science Foundation of China under Grant Nos 11174137, 11474215 and 21204058, the Natural Science Foundation for the Youth of Jiangsu Province under Grant No BK20130284, and the Priority Academic Program Development of Jiangsu Higher Education Institutions.

**Corresponding author. Email: dongwen@suda.edu.cn; wengyuyan@suda.edu.cn

© 2017 Chinese Physical Society and IOP Publishing Ltd

the deposition process started automatically and immediately. The WO_3 thin film (200 nm) was deposited on the FTO substrate (0.5 Å/s). To attain TiO_2-WO_3 composites, E-beam evaporations of 10 nm, 20 nm and 30 nm thin films were performed at a base pressure of about 1×10^{-4} Pa and a constant deposition rate of 0.5 Å/s. After deposition, heat treatments were conducted in the Nabertherm furnace where the samples were heated at the rate of 3℃/min up to 500℃ and maintained the temperature for 2 h, then cooled down to the ambient temperature.

The crystalline phases of the samples were examined using an x-ray diffraction (XRD) from 20° to 80° (X'Pert-Pro MPD). The samples surface morphologies were characterized via the field emission scanning electron microscopy (SEM, SU8010) and atomic force microscopy (AFM, MFP-3D-SA). The cross sectional images of the composite film were characterized via the transmission electron microscopy (TEM, Tecnai G220 S-TWIN, FEI). The absorption spectra of nanostructures were measured by a Perkin–Elmer Lambda 750 UV/NIR spectrometer. The EIS measurement was also performed at 0.5 V (V.vsAg/AgCl) to further elucidate the role of TiO_2 in the photogenerated charge separation and transport properties.

The photocurrent measurements were conducted in the three-electrode electrochemical workstation (CHI-660E, Chenhua instrument Co. Ltd). The WO_3 film and TiO_2-WO_3 composites as the working electrode were exposed under irradiation with the area 0.25 cm^2. The Pt wire and the Ag/AgCl electrode were used as a counter and reference electrodes, respectively. The coated side (including WO_3 and TiO_2-WO_3 composites) was immersed in an electrolyte aqueous solution of Na_2SO_4 (0.5 mol/L, PH=7), illuminated under the UV and the visible light via placing a long pass filter (cut-on wavelength 420 nm) in the irradiation path, which is derived from the 100 W xenon lamp source. The incident photon to current conversion efficiency (IPCE) of the different wavelengths by cutting on the filters was used to obtain the irradiation of desired wavelengths.

Figures 1(a) and 1(b) show the transmission electron microscopy image of the typical TiO_2-WO_3 heterojunction system. From the cross-sectional image (Fig. 1(a)), it is found that the whole structure is composed of (from bottom to top) a fluorine-doped tin oxide (FTO) substrate coated with a WO_3 film followed by a thin TiO_2 layer. The thicknesses of WO_3 and TiO_2 layers are about 200 nm and 20 nm, respectively. The high-resolution TEM image in Fig. 1(b) shows that the lattice spacing is 0.35 nm, which corresponds to the (101) and (10$\bar{1}$) planes of anatase TiO_2. Alongside TiO_2, the lattice spacing of 0.38 nm corresponds to the (002) planes of monoclinic WO_3.

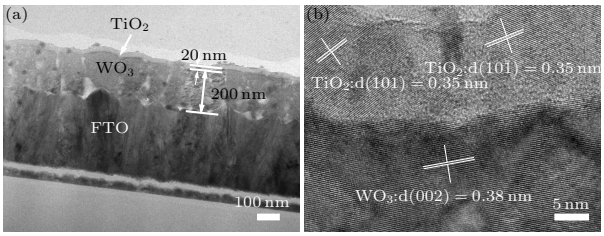

Fig. 1. (a) Cross-sectional TEM and (b) HRTEM images of TiO_2-WO_3 composite films.

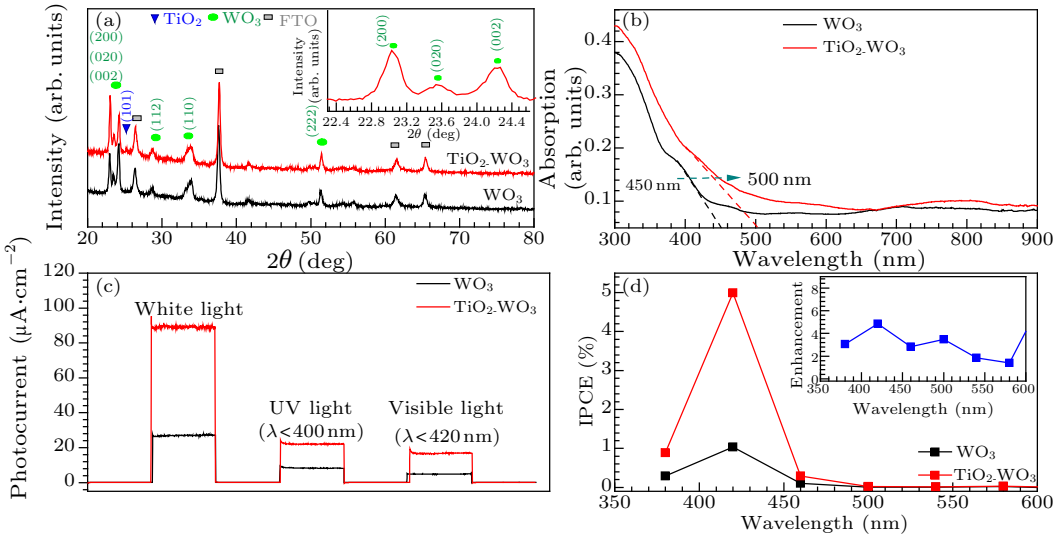

Fig. 2. (a) XRD patterns, (b) UV-vis absorption spectrum, (c) photocurrent density, and (d) IPCE action spectrum of pure WO_3 (black line) and TiO_2-WO_3 composite films (red line).

The crystalline phase composition as obtained by thin films was analyzed by x-ray diffraction. Figure 2(a) presents the XRD patterns for the pure WO_3 films and the 20-nm-TiO_2-WO_3 composite film. It can be seen that a series of characteristic peaks are noted in the XRD pattern of the WO_3 film after 500℃ sintering for 2 h, which are related to the (200), (020), (002), (112), (110), (121), (222) and (401) crystallo-

graphic planes of monoclinic WO_3 (JCPDS card No. 83-950). In terms of the TiO_2 loaded WO_3 composite film, it can be found that there is a weak peak at 25.3°, which corresponds to the (101) of anatase TiO_2. Additionally, any other characteristic peaks belonging to TiO_2 could not be detected in these heterojunction systems. We think that the main reason may ascribe to the high crystallinity of WO_3 phases, thus the dominant peaks of the 20-nm-TiO_2-WO_3 composite film appear. The peaks of the FTO structure were also indexed obviously. These results indicate that the incorporation of TiO_2 on the surface of the WO_3 film was successfully achieved using our proposed method and the existence of TiO_2 did not change the crystalline structure of the WO_3 film.

Figure 2(b) exhibits the typical absorption spectrum of the pure WO_3 film and the composite sample. The absorption edge of the pure WO_3 film is about at 450 nm. It is interesting that the absorption edge of the 20-nm-TiO_2-WO_3 heterojunction structure is slightly shifted 50 nm toward to the visible region, which is about 500 nm. We think the phenomenon that occurred can be attributed to two reasons: one is that the content of TiO_2 on the surface of the WO_3 film is low, which has a small effect on the absorption edge of WO_3. The other is the TiO_2 grains changing the surface roughness of the TiO_2-WO_3 composite films resulting in the enhancement of the absorption of the visible light, though the band energy gap of TiO_2 is 3.2 eV.

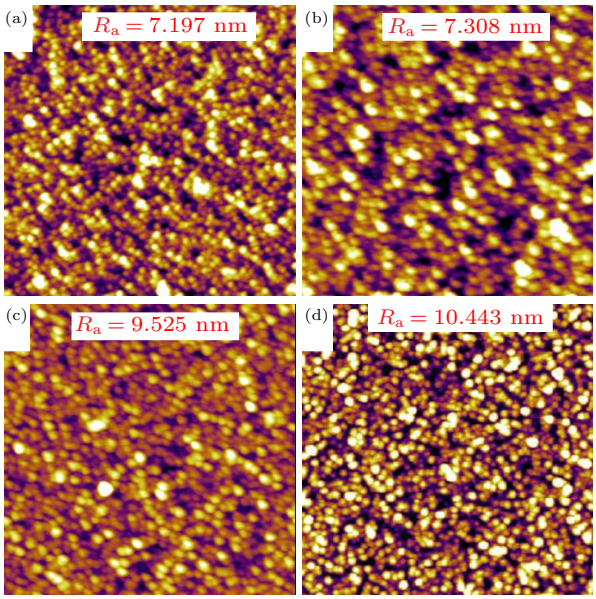

Fig. 3. AFM images of pure (a)WO_3 film, (b) 10-nm-TiO_2-WO_3 composite films, (c) 20-nm-TiO_2-WO_3 composite films, and (d) 30-nm-TiO_2-WO_3 composite films.

The surface morphologies of the pure WO_3 and the TiO_2-WO_3 composite films were observed by an atomic force microscope (AFM). As shown in Fig. 3, the rms roughness of the pure WO_3, 10-nm-TiO_2-WO_3, 20-nm-TiO_2-WO_3 and 30-nm-TiO_2-WO_3 are found to be 7.197 nm, 7.308 nm, 9.525 nm and 10.443 nm, respectively, which indicate that the surface roughness of all the composite films increase with the thickness of TiO_2 films.

The photocurrent density measured for the pure WO_3 film and the TiO_2-WO_3 heterojunction sample under xenon lamp illumination at 1.0 V external potential versus RHE are illustrated in Fig. 2(c), respectively. It is seen from Fig. 2(c) that under simulation white light illumination, the photocurrent of the pure WO_3 film is about 25 $\mu A/cm^2$, which is similar to the results reported in the literature.[22] The photocurrent density for the prepared 20-nm-TiO_2-WO_3 composite structure reaches a value of $\sim$90 $\mu A/cm^2$, which is about 3.6 times the one on the WO_3 film. Obviously, a thin TiO_2 film leads to an enhancement of the photocurrent density. When the samples were illuminated under the UV light (<400 nm) and visible light (>420 nm), it can be observed that the trend of photocurrent changes is similar to the simulated white-light case. The photocurrent densities of the TiO_2-WO_3 composite structure are 2.5 and 4.0 times the one on the WO_3 film.

To verify the relation between the photocurrent and the absorption, measurements of the incident photon to current conversion efficiency (IPCE) are performed under 1.0 applied bias voltage versus RHE. The IPCE values are defined as IPCE=$1240R/\lambda$, where λ is the incident light wavelength (nm), and $R = I/J$ is the photoresponsivity, with I being the measured photocurrent density (mA/cm^2) and J being the incident light power density (mW/cm^2). An IPCE action spectrum for the pure WO_3 film and the TiO_2-WO_3 composite structure was measured, as shown in Fig. 2(d). It is clearly indicated that the TiO_2-WO_3 composite structure (line with circles) shows much higher IPCE values than the pure WO_3 sample (line with squares). The IPCE enhancement ratio of the 20 nm TiO_2-WO_3 composite nanostructure to the pure WO_3 film demonstrates that the enhancement is significant in the UV and visible light region and can reach a particular high factor of 5 at the wavelength 420 nm (inset in Fig. 2(d)). This phenomenon is consistent with the absorption of the composite nanostructure.

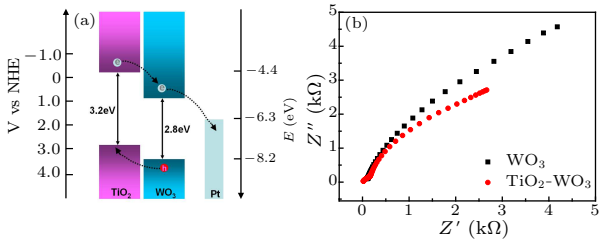

Fig. 4. (a) Schematic diagrams showing the energy band structure. (b) EIS measurement of the pure WO_3 film and the 20-nm-TiO_2 film loaded WO_3 composite films.

A possible mechanism for enhancement photocurrent density on the film loaded WO_3 composite structure electrode is given in Fig. 4. When the electrode

is exposed under Xe lamp illumination, the photons more than 3.2 eV can be absorbed by the thin TiO_2 film, while the transmitted part of the spectrum may be absorbed by the WO_3 film. Then the photogenerated electrons (e^-) and holes (h^+) obtained in both WO_3 and TiO_2 will migrate as shown in Fig. 4(a) because the conduction band energy level and the valence band energy level of WO_3 are lower than those of TiO_2. The whole process is as follows:[16,17,23] firstly, the photo-excited electrons can be transferred from the conduction band of TiO_2 to the conduction band of WO_3 and approach to the counter electrode. In the other aspect, the holes also transfer from the valence of WO_3 to the valence band of TiO_2 and effectively reach the electrolyte. As a result, the lifetime of electron-hole pairs may be prolonged, while the recombination of charge carriers can be suppressed in such a heterojunction. In addition, the TiO_2 thin film makes the surface roughness of the WO_3 film increase, which may lead to the quick photo-response. Hence, the overall photocurrent density of the WO_3 film can be increased significantly, by coupling different semiconductors, like TiO_2, having comparable band gaps.

To better understand the PEC performance, we performed an electrochemical impedance spectroscopy (EIS) measurement to elucidate the charge-transfer properties in different samples. The Nyquist impedance plots display one distinguishable semi-arc, whose diameters characterize the charge separation and transfer at the surface of the electrode.[24–26] The EIS Nyquist arc radius of 20 nm TiO_2-WO_3 composite films is smaller than that of WO_3 films, indicating a smaller electron transfer resistance at the surface of photo-electrodes, and a more effective separation of photogenerated electron-hole pairs and faster interfacial charge transfer are expected in the TiO_2-WO_3 composite structure.

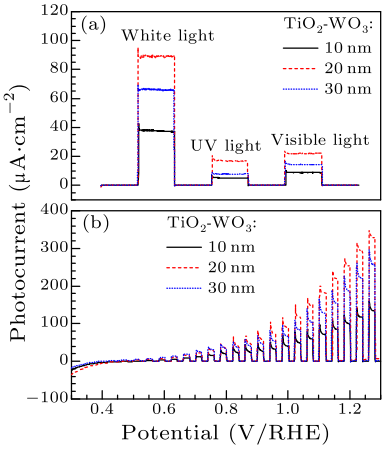

Fig. 5. Photocurrent density (a) and chopped-current-potential (I–V) curves (b) of TiO_2-WO_3 composite films with different thicknesses of TiO_2 films.

In the previous reports, the compositional ratio of WO_3 for the WO_3-TiO_2 heterostructures is important to the photocatalytic properties.[27,28] Thus in these studies, we think that the compositional ratio of TiO_2 is of critical importance for determining the photocatalysis activity of the supported semiconductor. In our case, we presented the photocurrent density of TiO_2-WO_3 composite films with different coverage areas of TiO_2 on the surface of WO_3 in Fig. 5(a), which were measured under illumination of the simulated light of the whole spectrum region, visible light and ultra-visible light under 1.0 V versus RHE. From this figure, it can be found that the photocurrent is about 37 $\mu A/cm^2$ under the illumination of simulation white light when the thickness of the TiO_2 film is 10 nm. Furthermore, the photocurrent of the 20 nm TiO_2 composite film illuminated by the same simulated white light reaches about 90 $\mu A/cm^2$.

In the case of the optimum coverage of the WO_3 surface by a thin TiO_2 film, the two metal oxide absorb incident photons generate the charge carriers, which may experience the interfacial carrier transfer process, thereby enhancing the photocurrent in the whole wavelength region.

When the thickness of TiO_2 exceeds 20 nm, the photocurrent density of composite samples decreases. The reason can be such that covered TiO_2 can influence the absorption of the WO_3 film, ensuring less electron-hole pair generations, thus leading to the decline of the photocurrent, although the TiO_2 layer in contact with the WO_3 film can promote the charge carriers transfer and restrain the recombination of charge carriers. Under visible light and UV irradiation, the trend of photocurrent changes is similar as compared with the simulated white light. Figure 5(b) shows a set of chopped current-potential (I–V) curves of the different samples under 100 W Xe-lamp illuminations in 0.1 M Na_2SO_4 solution. At 1.25 eV applied potential versus RHE, the photocurrent value of 20-nm-TiO_2-WO_3 composite films reaches about 0.3 mA/cm^2.

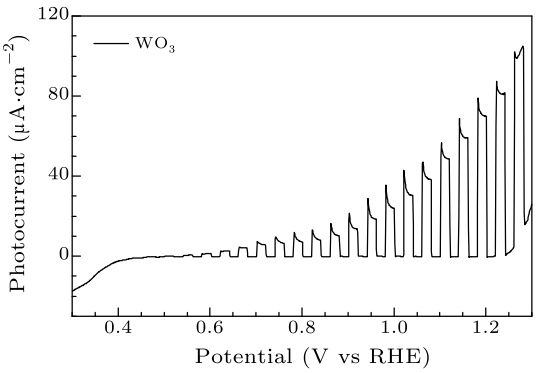

Fig. 6. PEC chopped-current-potential (I–V) curves of the pure WO_3 under 100 W Xe-lamp illuminations in 0.1 M Na_2SO_4 solution. The samples were scanned at 2 mV/s from left to right potentials.

However, from Fig. 6, we can find that the pure WO_3 film is broken down at 1.25 V versus RH, which indicates that the TiO_2 layer can promote the stability of the sample. The photocurrents of different samples

almost correspond to i–t curves. Interestingly, when the thickness of TiO_2 increases, the onset of photocurrent negatively shifts from 0.56 V to 0.44 V versus RHE because the onset voltage of TiO_2 is more negative than WO_3.

In summary, the TiO_2-WO_3 composite sample has been fabricated by a simple, robust and cost-effective method involving E-beam vapor deposition and thermal annealing. It is experimentally demonstrated that the prepared composite structures could strikingly improve photoelectron-chemical properties, especially such as photocurrent. Furthermore, the composite structures are optimized by varying the thickness of the initial TiO_2 film to obtain the highest photocurrent generation efficiency. We believe that the sophisticated phenomenon is attributed to the existence of the heterojunction, which results in the efficient charge carriers' separation, transfer process, and a lower recombination of electron-hole pairs.

References

[1] Kudo A and Miseki Y 2009 *Chem. Soc. Rev.* **38** 253
[2] Parida K M et al 2010 *J. Mater. Chem.* **20** 7144
[3] Biswal N et al 2011 *Int. J. Hydrogen Energy* **36** 13452
[4] Mor G K et al 2005 *Nano Lett.* **5** 191
[5] Nowotny J et al 2007 *Int. J. Hydrogen Energy* **32** 2609
[6] Alexander B D et al 2008 *J. Mater. Chem.* **18** 2298
[7] Butler M A 1977 *J. Appl. Phys.* **48** 1914
[8] Wang H L et al 2014 *Chem. Soc. Rev.* **43** 5234
[9] Hong S J et al 2011 *Energy Environ. Sci.* **4** 1781
[10] Liu L M et al 2014 *ACS Appl. Mater. Interfaces* **6** 5629
[11] Ma J F et al 2015 *Ceram. Int.* **41** 2050
[12] Castro I A et al 2014 *CrystEngComm* **16** 1514
[13] Patrocinio A O T et al 2014 *ACS Appl. Mater. Interfaces* **6** 16859
[14] Li S X et al 2015 *J. Mater. Chem.* A **3** 5467
[15] Hiroshi I et al 2004 *Vacuum* **74** 625
[16] Yang J K et al 2013 *Catal. Today* **201** 195
[17] Park H et al 2012 *Catal. B-Environ.* **115** 74
[18] Fujishima A and Honda K 1972 *Nature* **238** 37
[19] Shiyanovskaya A and Hepel M 1999 *J. Electrochem. Soc.* **146** 243
[20] Song K et al 2001 *Chem. Mater.* **13** 2349
[21] Tatsuma T et al 2001 *Chem. Mater.* **13** 2838
[22] Wang H L et al 2000 *J. Phys. Chem.* B **104** 5686
[23] Yu H T and Quan X 2009 *Progr. Chem.* **2** 406 (in Chinese)
[24] Hagfeldt A and Gratzel M 1995 *Chem. Rev.* **95** 49
[25] Woodhouse M et al 2005 *Chem. Mater.* **17** 4318
[26] Leng W H et al 2005 *J. Phys. Chem.* B **109** 15008
[27] Wang T et al 2014 *J. Power Source* **248** 510
[28] Liu Y et al 2012 *Appl. Catal.* A **433** 81